



HONOURS DISSERTATION

CHRISTOPHER JAMES THOMSON
2012

THIS THESIS WAS SUBMITTED AS PART OF THE REQUIREMENT FOR
THE MENG. DEGREE IN ENGINEERING.

ABSTRACT

The objective of this thesis is to determine a general technique for converting continuous potentials to equivalent discrete potentials. Discrete potentials have many desirable properties.

CONTENTS

Abstract	2
Nomenclature	7
Acknowledgements	8
1 Introduction	9
2 Molecular Models	10
2.1 Classical Mechanics	10
2.1.1 Validity of Classical Mechanics	10
2.1.2 Newton's Second Law of Motion	10
2.2 Continuous Potentials	11
2.3 Discrete Potentials	13
3 Molecular Dynamics	15
3.1 Force-driven Simulators	15
3.1.1 Initialisation	16
3.1.2 Integrators	16
3.1.3 Periodic Boundary Conditions	18
3.1.4 Thermostat	19
3.1.5 Optimisation	19
3.2 Event-Driven Simulators	21
3.2.1 Introduction	21
3.2.2 Collision Time Prediction	22
3.2.3 Collision Dynamics	23
4 Measuring Thermodynamic Properties	25
4.1 Introduction	25
4.2 Units	26
4.3 Energy	26

4.4	Temperature	27
4.5	Pressure	28
4.6	$g(r)$	29
4.7	$g(r)$ to pressure and temperature	29
4.8	long range corrections	29
5	From Continuous to Discontinuous	30
6	Results	31
6.1	Benchmarking	31
6.1.1	Introduction	31
6.1.2	Force based code versus NIST and ESpReSSo	31
6.1.3	Event Driven	31
6.2	Chapela's dumb stepping and very good stepping versus force based. . .	31
6.3	Stepping in probability versus action	31
6.4	Hard core position	32
6.5	Temperature comparisons	32
6.5.1	Event-Driven Simulator	32
6.6	References	33
A	Derivation of Collision Dynamics for Stepped Potentials	36

Final word count:

LIST OF FIGURES

2.1	Plot of the Lennard-Jones potentia	12
2.2	Plot of the force between a pair of Lennard-Jones particles separated by a distance r	13
3.1	Figure showing 2D periodic boundary conditions. Only the nearest 8 images (dashed) to the simulated system (solid) are shown.	18
4.1	Plot showing fluctuation of pressure ($P^* = P\sigma^3/\varepsilon$), kinetic energy per particle ($E_K^* = E_K/N\varepsilon$) and potential energy per particle ($U^* = U/N\varepsilon$). Results are from a force-driven simulation involving 864 particles, at a density $\rho^* = 0.9$ and temperature $\langle T \rangle = 1.497$. Values were collected every 10 timesteps where each timestep was $\Delta t = 0.005$	26

LIST OF TABLES

4.1	Table of reduced forms of various quantities used in this dissertation [9]	27
6.1	Comparison of results obtained by the event-driven simulator with literature values. t_{avg} is the average time between collisions, $\langle \hat{\mathbf{r}} \cdot \Delta \mathbf{v} \rangle_{coll}$ is the average momentum transfer per collision, and D is the coefficient of diffusion.	32
6.2	Comparison of results obtained by the event-driven simulator with literature values using stepped potentials. Numbers in parenthesis indicate the uncertainty in the final digit.	33

NOMENCLATURE

Acronyms/Terminology

FCC Face Centered Cubic, 16

MD Molecular Dynamics, 10

ACKNOWLEDGEMENTS

I would like to dedicate this work to..

INTRODUCTION

Process simulation packages have become an integral part of chemical engineering design. Central to these simulation software packages is the ability to calculate thermodynamic and transport properties of fluids quickly and accurately. Many modern processes rely on molecular scale effects... (Absorption, membrane technology (reverse osmosis), catalysis)....

To better understand these large scale systems, we need to improve our understanding of the smaller scales. Experiments are hard, can't hold a ruler up to a molecule, everything is too fast, too small to see. (X-ray crystallography). theory is hard, lots of molecules, can't solve even three molecules motion analytically (need cite). simulations are great, don't try to solve analytically. Since 50's (alder wainwright), computers are faster, modern sims are amazing.

At the heart of these simulations are models for the atoms and molecules involved. There are two classes of models, discrete and continuous.

In chapter ??, the something is discussed

MOLECULAR MODELS

In this chapter, the models used for molecular dynamics (MD) are discussed. There are two major types of potentials: continuous and discrete potentials, both are important to molecular dynamics. The solution to both relies on the use of classical mechanics to describe the motion of particles.

2.1 Classical Mechanics

2.1.1 Validity of Classical Mechanics

The underlying assumption behind many molecular dynamics simulations is that the particles move according to the laws of classical mechanics. Strictly, due to their size and speed, atom and molecules should be treated using quantum mechanics. However molecular dynamics makes a couple of assumptions that allow these quantum mechanical effects to be ignored.

The first is the Born-Oppenheimer Approximation which allows the motion of electrons and the nucleus to be treated separately. Since the nucleus is much larger than the electrons and hence less affected by quantum mechanics, it is treated as a classical particle. The electrons on the other hand are represented using a potential [11].

The second assumption is that any quantum mechanical effects should cancel out. Molecular dynamics is rarely interested in the motion of a single particle, it is more concerned with the statistical average of every particle.

These assumptions are usually valid unless very light atoms (such as hydrogen or helium) are being simulated or the particles are vibrating at very high rates [6].

2.1.2 Newton's Second Law of Motion

The fundamental identity of newtonian mechanics is Newton's Second Law of Motion (equation (2.1.1)). This equation allows the prediction of a particle's trajectory pro-

vided that an initial position and velocity is known; and the forces acting on that particle can be calculated for any position or velocity.

$$\mathbf{F} = m\mathbf{a} \quad (2.1.1)$$

If a force depends only on the position of a particle it is known as a conservative force. Almost all forces considered in molecular dynamics are of this type because atoms or molecules do not lose energy due to friction or any other dissipative process.

Conservative forces can be of one of two types. The first are forces that depend on a particle's absolute position, such as gravity. However gravity is usually disregarded in MD as atoms and molecules have such low masses that gravity has very little effect.

The second and most important type are intermolecular forces that depend on position relative to other particles. Usually only the forces between pairs of particles are considered, therefore the total force acting on a particle i is the sum of the forces between i and every other particle j . This pairwise summation of forces is shown in equation (2.1.2), where N is the total number of particles in the system.

$$\mathbf{F}_i = \sum_{j \neq i}^N \mathbf{F}_{ij} \quad (2.1.2)$$

Force calculations are limited to pairs as this is simpler, but there are examples of n -body forces such as equation (2.1.3) [24]. Here the force between particles i and j is split into a repulsive force (\mathbf{F}_R) and an attractive force (\mathbf{F}_A). The coefficient in front of the repulsive force, a , is a range limiting term, while the coefficient b , is the bond order. This describes the environment the particles are in, and strengthens or weakens the attractive force appropriately.

$$\mathbf{F}_{ij} = a\mathbf{F}_R + b\mathbf{F}_A \quad (2.1.3)$$

The intermolecular forces used in molecular dynamics are frequently described using a potential. Provided that the force is conservative, it can be calculated from its potential by equation (2.1.4). Here ∇ denotes the gradient of the potential is the partial differential of the potential in each orthogonal direction.

$$\mathbf{F} = -\nabla\mathcal{U} \quad (2.1.4)$$

2.2 Continuous Potentials

A very popular potential used in molecular dynamics simulations is the Lennard-Jones potential [15] shown in figure 2.1 and equation (2.2.1) as it is simple yet gives comparable results to experimental values.

$$U(r) = 4\epsilon \left[\left(\frac{\sigma}{r} \right)^{12} - \left(\frac{\sigma}{r} \right)^6 \right] \quad (2.2.1)$$

In equation (2.2.1), ϵ is the depth of the energy well, while σ is the distance where the potential between two particles is zero.

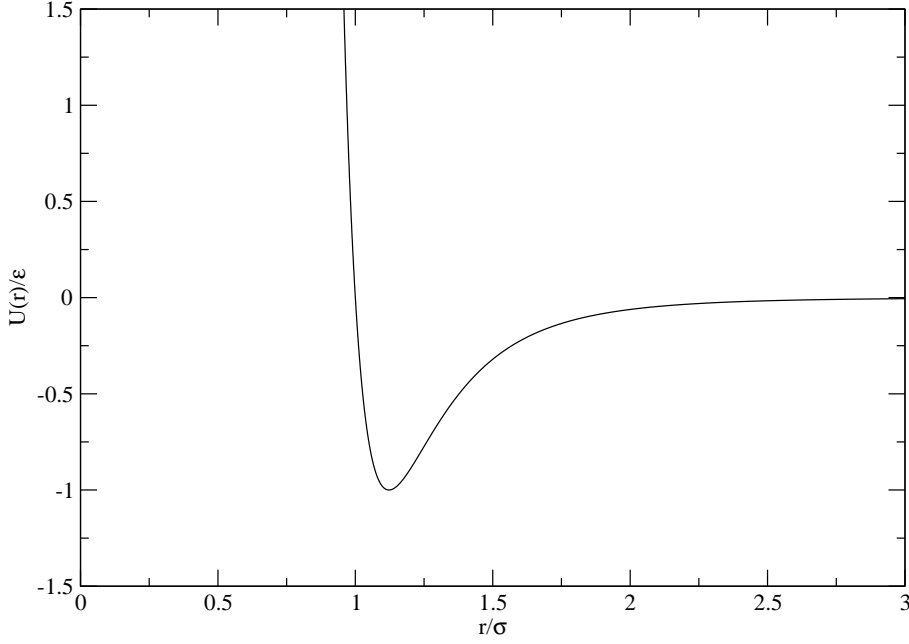


Figure 2.1: Plot of the Lennard-Jones potential

The power 12 term, $\left(\frac{\sigma}{r}\right)^{12}$ gives the potential the repulsive core caused by overlapping electron shells, while the power 6 term, $\left(\frac{\sigma}{r}\right)^6$, represents the attractive Van der Waals forces. The force between two Lennard-Jones particles is shown in figure 2.2.

The Lennard-Jones potential is even part of more complex potentials such as equation (2.2.2) [17]. Here the Lennard-Jones potential is used to represent Van der Waals forces while Coulomb's Law ($\frac{q_i q_j}{r_{ij}}$) is modelling longer range electrostatic interactions. The first four terms are constraints on bond movements (stretching, angle bending, "dihedral angle" motion, and out of plane movement of rings respectively).

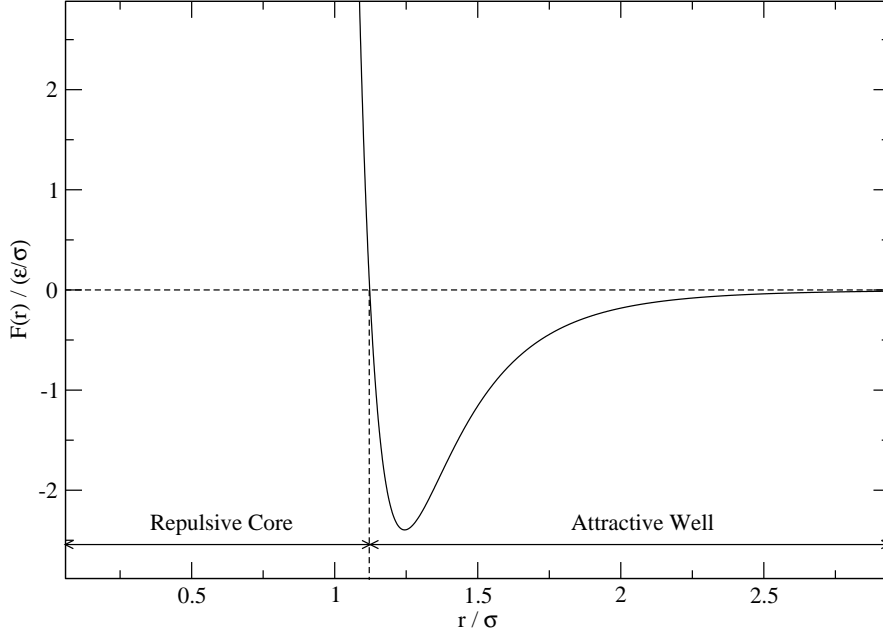


Figure 2.2: Plot of the force between a pair of Lennard-Jones particles separated by a distance r

$$\begin{aligned}
 \mathcal{U} = & \sum_{\text{bonds}} k_b (r - r_0)^2 + \sum_{\text{angles}} k_\theta (\theta - \theta_0)^2 \\
 & + \sum_{\text{dihedrals}} k_\chi [1 + \cos(n\chi - \delta)] + \sum_{\text{improper}} k_\psi (\psi - \psi_0)^2 \\
 & + \sum_{i=1}^{N-1} \sum_{j>i}^N \left\{ 4\epsilon \left[\left(\frac{\sigma}{r_{ij}} \right)^{12} - \left(\frac{\sigma}{r_{ij}} \right)^6 \right] + \frac{q_i q_j}{r_{ij}} \right\}
 \end{aligned} \tag{2.2.2}$$

2.3 Discrete Potentials

Discrete potentials differ from continuous potentials because they have discontinuities. The simplest discrete potential is that of the hard sphere.

Hard spheres were the first type of particles simulated [1] due to their relative simplicity. The potential for hard spheres is shown in equation (2.3.1), where σ is the diameter of the spheres.

$$\mathcal{U} = \begin{cases} \infty & \text{if } |\mathbf{r}_i - \mathbf{r}_j| < \sigma \\ 0 & \text{if } |\mathbf{r}_i - \mathbf{r}_j| > \sigma \end{cases} \tag{2.3.1}$$

The hard sphere potential can be elaborated upon by adding an attractive well outside the hard core. This square well potential takes the form of equation (2.3.2) [4], where λ is the outer radius of the core in terms of the hard core diameter σ .

$$\mathcal{U} = \begin{cases} \infty & \text{if } |\mathbf{r}_i - \mathbf{r}_j| < \sigma \\ -\varepsilon & \text{if } \sigma < |\mathbf{r}_i - \mathbf{r}_j| < \lambda\sigma \\ 0 & \text{if } |\mathbf{r}_i - \mathbf{r}_j| > \lambda\sigma \end{cases} \quad (2.3.2)$$

The square well potential is similar to the Lennard-Jones potential in that they have an attractive well, followed by a steep repulsive core, however the two give quite different simulation results.

Hence people have created better discrete potentials to model molecular interactions
Hard sphere,

square well -> compare to LJ

SPEAMD, PRIME

Lead out with the two methods used to simulate these potentials are quite different....

MOLECULAR DYNAMICS

3.1 Force-driven Simulators

In order to compare the effectiveness of step potentials a set of comparison results from a continuous potential is needed. The method to simulate a continuous potential is given in this section.

Force-driven (or time driven) simulators are the most popular method of simulating particles due to their relative simplicity and ability to handle continuous potentials. Simulators of this kind were pioneered by Rahman [20] who predicted physical properties of liquid argon using a Lennard-Jones potential with reasonable accuracy.

The distinguishing feature between force-driven and event-driven simulators is the way in which they move through time. During force-based simulations particles' positions and velocities are calculated at uniform intervals of time, Δt using the forces acting on the particles. These newly calculated values are then used to predict the next set of particle positions. This is then repeated over the desired simulation time.

The general algorithm for a force driven simulator is as follows.

1. Initialisation
2. Calculate particles' future positions
3. Calculate the forces acting on the particles
4. Calculate the future velocities of particles
5. Run thermostat (if enabled)
6. Measure properties
7. Repeat steps 2-6 for the desired number of iterations

3.1.1 Initialisation

The particles are initialised in a Face Centered Cubic (FCC) structure. The use of the FCC lattice is common when simulating Lennard-Jones potentials as the first force-driven simulation [20] was carried out using liquid Argon which crystallises to a FCC lattice.

Particle velocities are assigned randomly from a Gaussian distribution with a mean, $\mu = 0$, and a standard deviation, $\sigma = \sqrt{T^*}$, where T^* is the desired reduced temperature. The velocities are then rescaled to ensure there net shift in linear momentum in any direction by applying (3.1.1) in each orthongonal direction.

$$v_i^{new} = v_i^{old} - \frac{1}{N} \sum_i^N v_i^{old} \quad (3.1.1)$$

3.1.2 Integrators

Predicting the particles' future positions require solving Newton's Second Law of Motion (equation 3.1.2), using forces calculated from the potential.

$$\mathbf{F} = m \frac{\partial^2 \mathbf{r}}{\partial t^2} \quad (3.1.2)$$

However, since acceleration is the second time derivative of position (velocity is the first time derivative), calculating the particle's future position results in solving a differential equation. In order to accomplish this numerical integrators are used.

The majority of numerical integrators are based on Taylor Series (equation 3.1.3).

$$\mathbf{r}(t + \Delta t) = \mathbf{r}(t) + \frac{\partial \mathbf{r}(t)}{\partial t} (\Delta t) + \frac{1}{2} \frac{\partial^2 \mathbf{r}(t)}{\partial t^2} \Delta t^2 + \frac{1}{3!} \frac{\partial^3 \mathbf{r}(t)}{\partial t^3} \Delta t^3 + \frac{1}{4!} \frac{\partial^4 \mathbf{r}(t)}{\partial t^4} \Delta t^4 + \dots \quad (3.1.3)$$

The simplest integrator is Euler's Method which is just the Taylor Series truncated after the acceleration term (equation 3.1.4).

$$\mathbf{r}(t + \Delta t) = \mathbf{r}(t) + \mathbf{v}(\Delta t) + \frac{1}{2} \mathbf{a} \Delta t^2 + \mathcal{O}(\Delta t^3) \quad (3.1.4)$$

However this method suffers from large errors and is highly unstable (i.e. it amplifies any errors) [9] and is therefore rarely used. The Verlet Integrator [25] improves upon Euler's method by combining the forward timestep with a reverse timestep (3.1.5a). This method is actually fourth order as the third (and first) derivative is cancelled out during its derivation. The Verlet integrator does not include an equation to calculate the future

velocity so the central difference used by Verlet is often used (3.1.5b).

$$\mathbf{r}(t + \Delta t) = 2\mathbf{r}(t) - \mathbf{r}(t - \Delta t) + \mathbf{a}(t)\Delta t^2 + \mathcal{O}(\Delta t^4) \quad (3.1.5a)$$

$$\mathbf{v}(t + \Delta t) = \frac{\mathbf{r}(t + \Delta t) - \mathbf{r}(t - \Delta t)}{2\Delta t} \quad (3.1.5b)$$

Integrators suffer from couple key failings that cause a systematic gain of energy known as “energy drift”. Firstly, integrators are based on infinite Taylor series which cannot be fully implemented, therefore they have to be truncated after a certain number of terms, this introduces an error. Secondly, integrators struggle to predict values of forces that have discontinuities in them, such as discrete potentials or discontinuities introduced by truncating potentials to improve simulator speed. There are a couple of types of integrators that try and reduce these problems.

The first method to improve the traditional integrator is the predictor-corrector integrator. These use a truncated Taylor series to calculate a predicted value for the future position and higher order time derivatives. The force is then calculated at this predicted position, then the difference between the predicted acceleration and the corrected acceleration calculated from the force is used to correct the position and time derivatives.

The most popular predictor-corrector integrator is that of Gear [7], using his 5th order algorithm. The predicted value for the i^{th} time derivative is shown in (3.1.6), and defining $\Delta \mathbf{a} = \mathbf{a}^C - \mathbf{a}^P$, the corrected time derivatives can be calculated using (3.1.7) with coefficients from (3.1.8).

$$\frac{\partial^i}{\partial t^i} \mathbf{r}^P(t + \Delta t) = \sum_{k=i}^n \frac{1}{k!} \frac{\partial^i}{\partial t^i} \mathbf{r}(t) \Delta t^k \quad (3.1.6)$$

$$\frac{\partial^i}{\partial t^i} \mathbf{r}^C(t + \Delta t) = \frac{\partial^i}{\partial t^i} \mathbf{r}^P(t + \Delta t) + \frac{c_i}{\Delta t^i} \left(\frac{\Delta t^2}{2} \Delta \mathbf{a} \right) \quad (3.1.7)$$

$$c_0 = \frac{3}{16}, \quad c_1 = \frac{251}{360}, \quad c_2 = 1, \quad c_3 = \frac{11}{18}, \quad c_4 = \frac{1}{6}, \quad c_5 = \frac{1}{60} \quad (3.1.8)$$

The Gear’s algorithm, while more accurate at short timesteps than Verlet’s integrator [9], suffers at long timesteps and is computationally more expensive.

The other method used to try and mitigate the failings of other types of integrator is the symplectic integrator. These have the useful property in that they, on average, conserve energy [10]. The most common symplectic integrator used in MD is the Velocity Verlet Integrator [23] shown in (3.1.9).

$$\mathbf{r}(t + \Delta t) = \mathbf{r}(t) + \mathbf{v}(t)\Delta t + \frac{1}{2}\mathbf{a}(t)\Delta t^2 + \mathcal{O}(\Delta t^4) \quad (3.1.9a)$$

$$\mathbf{v}(t + \Delta t) = \mathbf{v}(t) + \frac{\mathbf{a}(t) + \mathbf{a}(t + \Delta t)}{2}\Delta t \quad (3.1.9b)$$

The popularity of the Velocity Verlet is due to its computational simplicity and its accuracy and stability at relatively long timesteps. It can even be expanded[12] to maintain its accuracy and stability at very long timesteps at a small extra computational cost. However the Velocity Verlet cannot be used in systems that do not conserve energy, ie systems with dissipative forces.

Since in this disseration all forces considered are conservative the Velocity Verlet integrator is used.

3.1.3 Periodic Boundary Conditions

When simulating a system it is necessary to have a boundary to prevent the particles from moving away from each into infinity. However solid walls have a large effect on the properties of a system so an alternative method is needed. Since some of the earliest MD simulations [2] have used periodic boundary conditions to solve this problem.

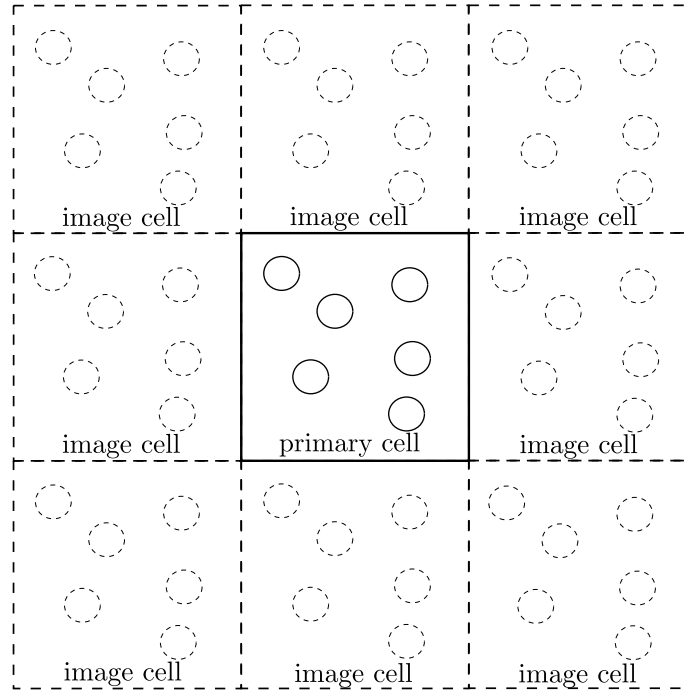


Figure 3.1: Figure showing 2D periodic boundary conditions. Only the nearest 8 images (dashed) to the simulated system (solid) are shown.

The concept behind periodic boundary conditions is to create a pseudoinfinite system made up of tessellated images of the simulated system (as shown in figure 3.1). When

a particle leaves the primary cell, its image enters from the opposite side. This ensures mass is conserved in each cell. This, however, brings the problem of particles being able to interact with multiple images of another particle, or even with themselves. The minimum image criterion is used to ensure particles only interact with the closest image of another particle.

3.1.4 Thermostat

All simulations in this dissertation used the canonical NVT ensemble, i.e. the number of particles, N ; the volume of the system, V and the temperature, T were kept constant during the simulation. While keeping the number of particles and system size constant is simple, controlling the temperature is more complex.

The simplest method for controlling the temperature is to rescale the particle velocities to match the desired temperature using equation (3.1.10).

$$\mathbf{v}_{\text{new}} = \mathbf{v}_{\text{old}} \sqrt{\frac{T_{\text{desired}}}{T_{\text{current}}}} \quad (3.1.10)$$

However this does not allow energy fluctuations that should exist in a NVT system, therefore an Andersen thermostat[3] is used. An Andersen thermostat works by colliding a random particle with a ghost particle at the desired temperature. In this force-driven simulation, this is achieved by reassigning the velocities of 5% of particles from a Gaussian distribution at the correct temperature (similar to section 3.1.1).

3.1.5 Optimisation

Due to the time-consuming nature of computer simulations there are a number of techniques used to speed up simulations. Since the calculation of the forces on the particles is the most time-consuming part of force-driven simulations [6], almost all optimising techniques focus on this aspect.

The first technique to improve simulation speed is to truncate the potential. Since continuous potentials tend to zero as particles get further away from each other, significant time can be saved by selecting a cut-off radius at which the potential is taken to be zero. The form of a truncated potential is shown in equation (3.1.11). For the Lennard-Jones potential a cut-off radius of 3σ is used as $\mathcal{U}(3\sigma) = -0.00548\varepsilon$ and $F(3\sigma) = -0.0109\varepsilon/\sigma$ are both approximately 1% of the minimum values.

$$\mathcal{U}(r) = \begin{cases} \mathcal{U}(r) & \text{if } r \leq r_{\text{cut-off}} \\ 0 & \text{if } r > r_{\text{cut-off}} \end{cases} \quad (3.1.11)$$

While truncating the potential prevents the calculation of the forces it still requires the computation of the distance between particles. These extraneous calculations can be

eliminated by using a neighbour list.

There are two main types of neighbour list used in molecular dynamics simulations. The first is the use of Verlet lists [25], and this is the type used in this dissertation for the force-driven simulation. A Verlet list is a list of all the particles within a certain radius of a particle. If this list was updated every timestep, this would be no improvement on the original method, but by making the Verlet radius larger than the truncation radius, these list can be used for multiple timesteps. Haile [9] recommends using a Verlet radius of 3.3σ , and updating the list every 10 timesteps, and this is what was done in this dissertation.

Another method is to use cell-linked lists [19], this method involves dividing the system into a grid and only the particles in the same cell or a neighbouring cell are taken into account. This method can however be inefficient as the length of each cell must be at least the truncation cut-off radius wide to prevent particles being missed out. However this means a volume of $27r_{\text{cut-off}}^3$ (as in 3 dimensions each cell has 26 neighbours) are considered but only particles within the spherical volume $\frac{4}{3}\pi r_{\text{cut-off}}^3$ should be checked; this means the volume checked is over six times larger than it needs to be.

Mattson and Rice [18] improve this by reducing the length of each cell to less than the cut-off radius, but this results in more neighbouring cells having to be checked i.e. for a cell length of $0.5r_{\text{cut-off}}$ the nearest 124 (a $5 \times 5 \times 5$ grid) cells are considered neighbours. This means there is a compromise as smaller cells mean that less volume is checked, but also means the cell lists are made obsolete quicker and therefore have to be generated more frequently.

3.2 Event-Driven Simulators

Start off by pointing out that discontinuous potentials have discontinuities! Whats the force on these points? Infinity! Can't integrate over these discontinuities, but what about between them? We can solve $F=ma$, (solve it). We can then analytically integrate newton's equation of motion. We can then try to detect when a discontinuity occurs and treat them as they happen.

How do you solve what happens over a discontinuity? Conservation of momentum and energy (see appendix).

3.2.1 Introduction

Most molecular dynamics simulations use potentials to calculate the forces acting on particles (see section 2.1.2), however this is problematic when using discrete potentials. The gradient (and hence the force) is either infinite at the steps or zero between them.

Therefore a new technique for simulating these discrete potentials is needed. Since between the steps there is no force therefore the acceleration (and higher order time derivatives) are zero the Taylor series (equation (3.1.3)) can be reduced to equation (3.2.1).

$$\mathbf{r}(t + \Delta t) = \mathbf{r}(t) + \mathbf{v}(t)\Delta t \quad (3.2.1)$$

This leaves only the problem of simulating the point where the particles are at a step, but since, energy and momentum must be conserved, this too can be overcome (this is expanded upon in section 3.2.3). This method is known as event-driven molecular dynamics.

Though force-driven simulators are more popular the first MD simulation was done using an event-driven simulator by Alder and Wainwright [1]. Event-driven simulators differ from force-driven simulators in that they move through time by jumping from the point when a discontinuity occurs (known as a collision) to the next discontinuity. These collisions are taken to be instantaneous and only one can occur at any particular time.

The general algorithm for a event driven simulator shown below.

1. Initialisation
 - i. Initialise particles
 - ii. Initialise event list
 - iii. Initialise capture map
2. Find the next event
3. Process the event

4. Update the event list
5. Measure properties
6. Repeat steps 2-5 for the desired number of events

This algorithm is more complex than that for the force driven simulation especially when event-driven simulators generally have many different types of event.

3.2.2 Collision Time Prediction

The initialisation of the particles for the event-driven simulation is identical to that for the force-driven simulation. An event-driven simulator first must calculate the collision times between every pair of particles (provided the particles do collide), in order to select the earliest collision. For hard sphere simulations there are two conditions that must be satisfied in order for a collision to occur. Firstly, the particles must be moving towards each other and secondly, the particles must pass close enough to each other to collide. These conditions can be expressed mathematically in equations (3.2.2a) and (3.2.2b) respectively [9].

$$\mathbf{v}_{ij} \cdot \mathbf{r}_{ij} < 0 \quad (3.2.2a)$$

$$(\mathbf{v}_{ij} \cdot \mathbf{r}_{ij})^2 - v_{ij}^2(r_{ij}^2 - \sigma^2) \geq 0 \quad (3.2.2b)$$

The time to collision can then be calculated using the quadratic in equation (3.2.3). While there are two solutions, only the earliest collision (the negative root) needs to be considered. The second root gives the time when the particles leave after passing through each other which, for hard sphere, cannot happen.

$$\Delta t = \frac{(-\mathbf{v}_{ij} \cdot \mathbf{r}_{ij}) \pm \sqrt{(\mathbf{v}_{ij} \cdot \mathbf{r}_{ij})^2 - v_{ij}^2(r_{ij}^2 - \sigma^2)}}{v_{ij}^2} \quad (3.2.3)$$

Since $\mathbf{v}_{ij} \cdot \mathbf{r}_{ij}$ must be negative for the collision, there is the possibility of catastrophic cancellation [8], if $(\mathbf{v}_{ij} \cdot \mathbf{r}_{ij})^2 \gg v_{ij}^2(r_{ij}^2 - \sigma^2)$. Therefore it is advisable to use the positive root from the alternate form of the quadratic equation given in equation (3.2.4) [19].

$$\Delta t = \frac{r_{ij}^2 - \sigma^2}{(-\mathbf{v}_{ij} \cdot \mathbf{r}_{ij}) \mp \sqrt{(\mathbf{v}_{ij} \cdot \mathbf{r}_{ij})^2 - v_{ij}^2(r_{ij}^2 - \sigma^2)}} \quad (3.2.4)$$

When considering stepped potentials many of the same principles apply, except there are now two possible “collisions”. The first, when two particles enter a step is treated

identically to hard spheres. The other event, when the particles leave the step, is calculated using the second, later root of the quadratic. In order to prevent loss of numerical precision, the leaving time should be calculated using equation (3.2.5).

$$\Delta t = \begin{cases} \frac{r_{ij}^2 - \sigma^2}{(-\mathbf{v}_{ij} \cdot \mathbf{r}_{ij}) - \sqrt{(\mathbf{v}_{ij} \cdot \mathbf{r}_{ij})^2 - v_{ij}^2(r_{ij}^2 - \sigma^2)}}, & \text{if } \mathbf{v}_{ij} \cdot \mathbf{r}_{ij} > 0 \\ \frac{(-\mathbf{v}_{ij} \cdot \mathbf{r}_{ij}) + \sqrt{(\mathbf{v}_{ij} \cdot \mathbf{r}_{ij})^2 - v_{ij}^2(r_{ij}^2 - \sigma^2)}}{v_{ij}^2}, & \text{if } \mathbf{v}_{ij} \cdot \mathbf{r}_{ij} < 0 \end{cases} \quad (3.2.5)$$

3.2.3 Collision Dynamics

Once the time of the next collision is known, the particles can be moved to their new locations. Generally there is no external force applied to the particles in event-driven molecular dynamics, therefore the particles move in straight lines. Hence the particles' new positions can be calculated using equation (3.2.1).

The post-collision velocities of the colliding particles must now be calculated. The simplest collision between two particles is an elastic bounce, where the velocities and just exchanged along the separation vector between the two particles. The change in velocity during the collision for particles i and j is shown in equation (3.2.6).

$$\Delta \mathbf{v}_i = -(\mathbf{v}_{ij} \cdot \hat{\mathbf{r}}_{ij})\hat{\mathbf{r}}_{ij} \quad (3.2.6a)$$

$$\Delta \mathbf{v}_j = (\mathbf{v}_{ij} \cdot \hat{\mathbf{r}}_{ij})\hat{\mathbf{r}}_{ij} \quad (3.2.6b)$$

For stepped potential system, the collision dynamics are more complex. When two particles collide they must pay an energy “cost” to proceed through the step. This energy cost ΔU is the difference in the energy of the current step and the step the particles are going into, and is shown in equation (3.2.7).

$$\Delta U = U_{\text{next step}} - U_{\text{current step}} \quad (3.2.7)$$

If the kinetic energy of the particles is insufficient, the pair bounce off the step and the post-collision velocities are calculated using equation (3.2.6). However, if the particles can pay this cost i.e. the inequality (3.2.8) is true, then the particles can enter the step.

$$\frac{1}{4}m(\mathbf{v}_{ij} \cdot \hat{\mathbf{r}}_{ij})^2 > \Delta U \quad (3.2.8)$$

The change in the velocities of particles i and j after going through a step are shown in equation (3.2.9) where A is given in equation (3.2.10), the derivation of these equations is given in Appendix ???. If the particles are entering a step, the positive root of A is used, whereas if the particles are leaving a step it is the negative root that should be used.

$$\Delta \mathbf{v}_i = \frac{A}{m} \hat{\mathbf{r}}_{ij} \quad (3.2.9a)$$

$$\Delta \mathbf{v}_j = -\frac{A}{m} \hat{\mathbf{r}}_{ij} \quad (3.2.9b)$$

$$A = -\frac{m}{2} \left((\mathbf{v}_{ij} \cdot \hat{\mathbf{r}}_{ij}) \pm \sqrt{(\mathbf{v}_{ij} \cdot \hat{\mathbf{r}}_{ij})^2 - \frac{4}{m} \Delta U} \right) \quad (3.2.10)$$

MEASURING THERMODYNAMIC PROPERTIES

4.1 Introduction

Molecular dynamics is a useful tool to predict macroscopic properties of particles systems. Many of the identities and methods to measure these properties are derived in statistical mechanics. However, even when the system is at equilibrium, these properties fluctuate around a mean (see figure 4.1) therefore it is common to take time averages of these values. These time averages are denoted with angle brackets $\langle \rangle$, and the time average of a property, A , is shown in (4.1.1) [9].

$$\langle A \rangle = \lim_{t \rightarrow \infty} \frac{1}{t} \int_{t_0}^{t_0+t} A(\tau) d\tau \quad (4.1.1)$$

This time average can be calculated precisely in event-driven simulations for several properties such as pressure, kinetic energy and potential energy. These only change at collisions and therefore are constant for the time between the collision and can be calculated by (4.1.2).

$$\langle A \rangle = \frac{1}{t} \sum_{t_0}^{t_0+t} A(\tau) \Delta\tau \quad (4.1.2)$$

In force-driven simulators all properties change continuously and hence time averages cannot be calculated precisely, however approximations can be made. If properties are measured every uniform period of time, the time average can be approximated by equation (4.1.3), where M is the number of measurements taken.

$$\langle A \rangle = \frac{1}{M} \sum_1^M A(\tau) \quad (4.1.3)$$

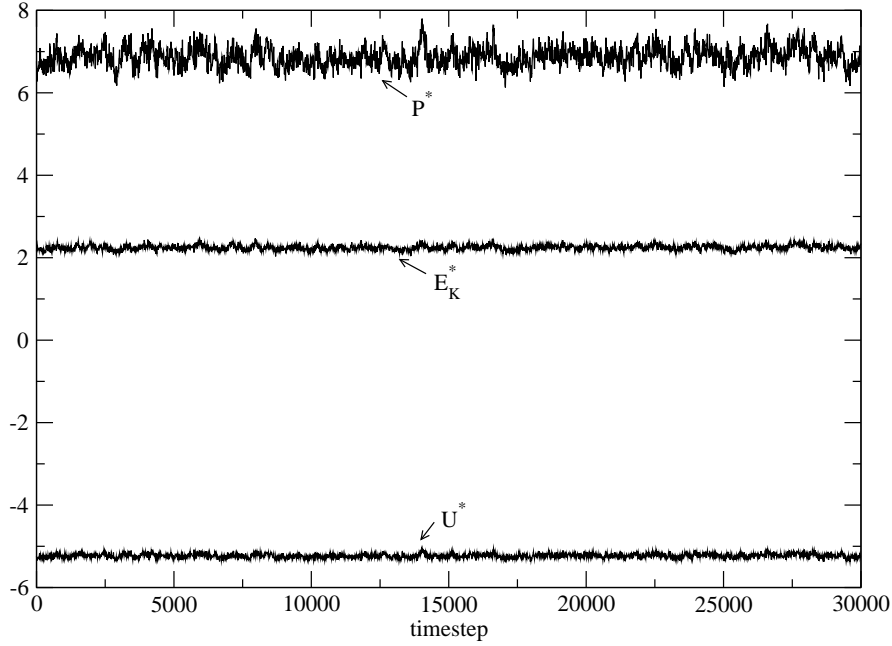


Figure 4.1: Plot showing fluctuation of pressure ($P^* = P\sigma^3/\varepsilon$), kinetic energy per particle ($E_K^* = E_K/N\varepsilon$) and potential energy per particle ($U^* = U/N\varepsilon$). Results are from a force-driven simulation involving 864 particles, at a density $\rho^* = 0.9$ and temperature $\langle T \rangle = 1.497$. Values were collected every 10 timesteps where each timestep was $\Delta t = 0.005$.

4.2 Units

In molecular dynamics simulations, properties are frequently measured in dimensionless forms [9]. These “reduced units” are usually denoted with an asterisk. In order to achieve this a number of fundamental dimensions are needed: a characteristic length σ , a characteristic energy ε , and the mass of one particle m . In the case of the Lennard-Jones potential, the characteristic length and energy are taken as: the distance of the root, and the depth of the attractive well respectively. A table of reduced forms are given in table 4.1.

4.3 Energy

Perhaps one of the most important properties to measure in MD simulations is the total internal energy of the system. For isolated systems, i.e. systems where mass or energy cannot enter or leave the system, this internal energy is the sum of kinetic and potential energy (equation (4.3.1)).

Table 4.1: Table of reduced forms of various quantities used in this dissertation [9]

Quantity	Reduced forms
Density	$\rho^* = N\sigma^3/V$
Energy	$E^* = E/\varepsilon$
Force	$F^* = F\sigma/\varepsilon$
Length	$r^* = r/\sigma$
Pressure	$P^* = P\sigma^3/\varepsilon$
Temperature	$T^* = kT/\varepsilon$
Time	$t^* = t/(\sigma\sqrt{m/\varepsilon})$
Velocity	$v^* = v\sqrt{m/\varepsilon}$

$$E = E_K + \mathcal{U} \quad (4.3.1)$$

The total kinetic energy in the system is the sum of the kinetic energy of each particle, as shown in equation (4.3.2).

$$E_K = \sum_i^N mv_i^2 \quad (4.3.2)$$

The potential energy of the system is the sum of the potential energy between every pair of particles (for a pairwise potential), and is shown in equation (4.3.3).

$$\mathcal{U} = \sum_{i < j} \mathcal{U}(r_{ij}) \quad (4.3.3)$$

Event-driven simulators strictly conserve energy, therefore the kinetic and potential energy can be measured at the beginning of the simulation and then updated whenever either changes e.g. when a collision occurs.

4.4 Temperature

The velocity distribution of particles is given by the Maxwell distribution [9], shown in equation (4.4.1), where k_B is the Boltzman Constant.

$$f(v_x)dv_x = \sqrt{\frac{m}{2\pi k_B T}} e^{-\frac{mv_x^2}{2k_B T}} \quad (4.4.1)$$

This is the form of a Gaussian distribution and it can be shown [14] that the mean square velocity in any direction is as shown in equation (4.4.2).

$$\overline{v_x^2} = \frac{k_B T}{m} \quad (4.4.2)$$

Making the assumption that the velocity distribution is the same in each direction, the temperature can be expressed as equation (4.4.3), by taking the average temperature in each direction.

$$T^* = k_B T = \frac{mv^2}{3N} = \frac{2}{3N} E_K \quad (4.4.3)$$

This allows the calculation of the temperature from the kinetic energy of the system.

4.5 Pressure

The pressure in a molecular dynamics simulation is calculated using the virial equation of state (equation (4.5.1)) [14].

$$\frac{PV}{Nk_B T} = 1 + B_2 \rho + B_3 \rho^2 + B_4 \rho^3 + \dots + B_n \rho^{n-1} \quad (4.5.1)$$

The coefficients, $B_2, B_3, B_4, \dots, B_n$ are known as the second, third, etc. virial coefficients. Values for these virial coefficients are available in the literature for common potentials such as hard spheres [13] or Lennard-Jones [21]. Physically these coefficients represent the contribution to the pressure by two, three, etc particles interacting, and since most potentials are pairwise the pressure contribution is truncated at the second virial coefficient, the form of which in three dimensions is given in equation (4.5.2) [22].

$$B_2 = -2\pi \int_0^\infty (e^{U(r)/kT} - 1) r^2 dr \quad (4.5.2)$$

However these virial coefficients do not apply to molecular dynamics simulations that use periodic boundary conditions [9], therefore an alternative method is required.

Using kinetic theory and measuring momentum flux during the simulation an expression for the second virial coefficient can be created for both simulation methods. In force driven simulations, the second virial can be calculated using equation (4.5.3) [9].

$$B_2 \rho = \frac{1}{3NkT} \left\langle \sum_{i < j} \mathbf{F}_{ij} \cdot \mathbf{r}_{ij} \right\rangle \quad (4.5.3)$$

Calculating the pressure in event-driven simulators is more complex due to the lack of forces in the simulation, however by keeping track of the momentum flux at each collision an average pressure can be calculated using equation (4.5.4)[16]. Here N_{coll} is the total number of collisions during the time t .

$$B_2 \rho = \frac{m}{3} \frac{N_{\text{coll}}}{Nt} \langle \mathbf{r}_{ij} \cdot \Delta \mathbf{v}_i \rangle_{\text{coll}} \quad (4.5.4)$$

4.6 $g(r)$

4.7 $g(r)$ to pressure and temperature

4.8 long range corrections

FROM CONTINUOUS TO DISCONTINUOUS

State the case why we want to run discontinuous systems, the advantages (fast, extremely stable-> infinitely hard potentials, and disadvantages (underdeveloped set of potentials in the literature, complex algorithm). These disadvantages can be overcome by writing a good general EDMD program and finding a general method to convert the hard work in soft potentials to stepped potentials.

RESULTS

6.1 Benchmarking

6.1.1 Introduction

After a MD simulator has been created it is necessary to compare its results with those generated by others, to verify that the simulator works correctly.

6.1.2 Force based code versus NIST and ESpReSSo

6.1.3 Event Driven

Event driven codes are significantly more complex than time-stepping codes, so we need more tests

HARD SPHERES v LEO

Stepped Potential of Chapela

6.2 Chapela's dumb stepping and very good stepping versus force based.

Show that dumb stepping doesn't work, show how good chapela's results actually are when he tries. Proves this is possible.

6.3 Stepping in probability versus action

Hard cores dominate the freezing behaviour (see Alder and Wainwrights famous paper) and therefore for high density pressure etc. but the stepping in equal probability doesnt do this.

Table 6.1: Comparison of results obtained by the event-driven simulator with literature values. t_{avg} is the average time between collisions, $\langle \hat{\mathbf{r}} \cdot \Delta \mathbf{v} \rangle_{coll}$ is the average momentum transfer per collision, and D is the coefficient of diffusion.

ρ	t_{avg}		$\langle \hat{\mathbf{r}} \cdot \Delta \mathbf{v} \rangle_{coll}$		D	
	Simulator	Lue	Simulator	Lue	Simulator	Lue
0.3	0.3052	0.3052	1.775	1.772	0.53	0.55
0.4	0.1944	0.1942	1.776	1.773	0.341	0.359
0.5	0.13024	0.13031	1.774	1.7724	0.247	0.247
0.6	0.08966	0.08968	1.771	1.7721	0.169	0.173
0.7	0.0625	0.0625	1.773	1.776	0.114	0.113
0.8	0.04365	0.0436	1.772	1.772	0.064	0.065
0.9	0.03029	0.03024	1.773	1.772	0.033	0.0327

6.4 Hard core position

Try setting the inner step to infinite energy

Use barker henderson, an old attempt to make hard sphere match everything else. (too far out).

talk about probability of finding a particle in the core. Talk about sigma try out 3, 4, and 5.

6.5 Temperature comparisons

Show that chapelas solution gets worse faster than ours.

6.5.1 Event-Driven Simulator

The event-driven simulator was first tested running a hard sphere simulation before testing the more complex stepped potentials. A single 'step' with a energy requirement sufficiently large such that no particle could enter it. The simulation was run once at a range of densities using 864 particles at a reduced temperature of $T^* = 1$ for 5 million collisions, the results were compared with those of Lue [16] in table 6.1. The agreement between results is good and lies within statistical uncertainty. The largest discrepancies are in the values for the coefficient of diffusion at low densities which is probably due to Lue's values were obtained after 10 million collisions.

The simulator was then benchmarked using a step potential. The results were compared with Chapela et al [5] using their 'Case 6' steps. The simulation was run for 1.5 million collisions using 864 particles. Each simulation was run ten times and the mean values and standard deviations are given in table 6.2

Table 6.2: Comparison of results obtained by the event-driven simulator with literature values using stepped potentials. Numbers in parenthesis indicate the uncertainty in the final digit.

ρ	$\langle T \rangle$		$\langle U \rangle$		$\langle P \rangle$	
	Simulator	Chapela et al	Simulator	Chapela et al	Simulator	Chapela et al
0.85	0.719(3)	0.72	-6.04(7)	-5.80	-0.5(4)	0.54
0.85	1.339(8)	1.34	-5.130(9)	-5.14	4.08(4)	4.08
0.85	2.35(1)	2.35	-4.24(2)	-4.20	8.78(9)	8.86
0.85	3.37(2)	3.37	-3.48(2)	-3.49	12.90(9)	13.00
0.85	4.59(1)	4.60	-2.67(1)	-2.68	17.31(8)	13.43
0.75	0.811(2)	0.81	-5.095(3)	-5.08	-0.20(2)	-0.24
0.75	1.309(9)	1.31	-4.67(1)	-4.63	1.81(5)	1.84
0.75	2.49(1)	2.49	-3.88(1)	-3.82	5.80(4)	5.95
0.75	3.59(2)	3.59	-3.26(1)	-3.22	9.03(7)	9.20
0.65	1.309(8)	1.31	-4.081(8)	-4.06	0.80(3)	0.81
0.65	2.61(1)	2.61	-3.42(1)	-3.41	3.86(5)	3.89
0.65	3.79(1)	3.79	-2.926(9)	-2.94	6.34(7)	6.33

6.6 References

- [1] B. J. Alder and T. E. Wainwright. “Phase Transition for a Hard Sphere System”. In: *J. Chem. Phys.* 27 (1957), pp. 1208–1209. DOI: 10.1063/1.1743957.
- [2] B. J. Alder and T. E. Wainwright. “Studies in Molecular Dynamics. I. General Method”. In: *J. Chem. Phys.* 31 (1959), pp. 459–466. DOI: 10.1063/1.1730376.
- [3] H. C. Andersen. “Molecular dynamics simulations at constant pressure and/or temperature”. In: *J. Chem. Phys.* 72 (1980), pp. 2384–2393. DOI: 10.1063/1.439486.
- [4] J. A. Barker and D. Henderson. “Perturbation Theory and Equation of State for Fluids: The Square-Well Potential”. In: *J. Chem. Phys.* 47 (1967), pp. 2856–2861. DOI: 10.1063/1.1712308.
- [5] G. Chapela, L. E. Scriven, and H. T. Davis. “Molecular dynamics for discontinuous potential. IV. Lennard-Jonesium”. In: *J. Chem. Phys.* 91 (1989), p. 4307. DOI: 10.1063/1.456811.
- [6] D. Frenkel and B. Smit. *Understanding Molecular Simulations*. 2nd Edition. Academic Press, 2002. DOI: 10.1016/B978-012267351-1/50006-7.
- [7] C. W. Gear. *Numerical Initial Value Problems in Ordinary Differential Equations*. Ed. by George Forsythe. Prentice-Hall, 1971.

-
- [8] D. Goldberg. “What every computer scientist should know about floating-point arithmetic”. In: *ACM Comput. Surv.* 23.1 (1991), pp. 5–48. DOI: 10.1145/103162.103163.
 - [9] J M Haile. *Molecular Dynamics Simulation: Elementary Methods*. Wiley-Interscience, 1997.
 - [10] Ernst Hairer, Christian Lubich, and Gerhard Wanner. “Geometric numerical integration illustrated by the Stormer-Verlet method”. In: *Acta Numerica* 12 (2003), pp. 399–450. DOI: 10.1017/S0962492902000144.
 - [11] Ahren W. Jasper et al. “Non-Born - Oppenheimer Molecular Dynamics”. In: *Acc. Chem. Res.* 39.2 (2006), pp. 101–108. DOI: 10.1021/ar040206v.
 - [12] Z.M. Khakimov. “New integrator for molecular dynamics simulations”. In: *Comput. Phys. Commun.* 147 (2002), pp. 733–736. DOI: 10.1016/S0010-4655(02)00387-9.
 - [13] S. Labík, J. Kolafa, and A. Malijevský. “Virial coefficients of hard spheres and hard disks up to the ninth”. In: *Phys. Rev. E* 71 (2005), p. 021105. DOI: 10.1103/PhysRevE.71.021105.
 - [14] L.D. Landau and E.M. Lifshitz. *Statistical Mechanics*. 2nd. Vol. 5. Course of Theoretical Physics. Oxford: Pergamon, 1968.
 - [15] J.E. Lennard-Jones. “The Determination of Molecular Fields I & II”. In: *Proc. R. Soc. Lon. Ser-A* 106A (1924), pp. 441–477. DOI: 10.1098/rspa.1924.0081.
 - [16] L. Lue. “Collision statistics, thermodynamics, and transport coefficients of hard hyperspheres in three, four, and five dimensions”. In: *J. Chem. Phys.* 122.4 (2005), p. 044513. DOI: 10.1063/1.1834498.
 - [17] E. J. Maginn and J. R. Elliott. “Historical Perspective and Current Outlook for Molecular Dynamics As a Chemical Engineering Tool”. In: *Ind. Eng. Chem. Res.* 49 (2010), pp. 3059–3078. DOI: 10.1021/ie901898k.
 - [18] W. Mattson and B. M. Rice. “Near-neighbour calculations using a modified cell-linked list method”. In: *Comput. Phys. Commun.* 119 (1999), pp. 135–148. DOI: 10.1016/S0010-4655(98)00203-3.
 - [19] T. Pöschel and T. Schwager. *Computational Granular Dynamics: Models and Algorithms*. Springer, 2005.
 - [20] A Rahman. “Correlations in the Motion of Atoms in Liquid Argon”. In: *Phys. Rev.* 136 (1964), A405–A411. DOI: 10.1103/PhysRev.136.A405.
 - [21] A. J. Schultz and D. A. Kofke. “Sixth, seventh and eighth virial coefficients of the Lennard-Jones model”. In: *Mol. Phys.* 1007 (2009), pp. 2309–2318. DOI: 10.1080/00268970903267053.

- [22] J. M. Smith, H. C. Van Ness, and M.M. Abbott. *Introduction ot Chemical Engineering Thermodynamics*. 7th. New York: McGraw-Hill, 2005.
- [23] William C. Swope et al. “A computer simulation method for the calculation of equilibrium contants for the formation of physical clusters of molecultes: Application to small water clusters”. In: *J. Chem. Phys.* 76 (1982), pp. 637–649. DOI: 10.1063/1.442716.
- [24] J. Tersoff. “New empirical approach for the structure and energy of covalent systems”. In: *Phys. Rev. B* 37 (1988), pp. 6991–6999. DOI: 10.1103/PhysRevB.37.6991.
- [25] Loup Verlet. “Computer "Experiments" on Classical Fluids. I. Thermodynamical Properties of Lennard-Jones Molecules”. In: *Phys. Rev.* 159 (1967), pp. 98–103. DOI: 10.1103/PhysRev.159.98.

DERIVATION OF COLLISION DYNAMICS FOR STEPPED POTENTIALS

Considering a collision between particles i and j , each with mass, m with a step energy difference of ΔU , the conservation of momentum is shown in equation (A.0.1). Here the prime indicates post-collision values.

$$m\mathbf{v}_i + m\mathbf{v}_j = m\mathbf{v}'_i + m\mathbf{v}'_j \quad (\text{A.0.1})$$

The momentum change of each particle must occur along the separation vector between the two particles, which can be expressed by equation (A.0.2), where A is an arbitrary coefficient.

$$m\mathbf{v}_i - m\mathbf{v}'_i = -(m\mathbf{v}_j - m\mathbf{v}'_j) = -A\hat{\mathbf{r}}_{ij} \quad (\text{A.0.2})$$

Energy must also be conserved in the system so equation (A.0.3) must also apply. This can be rewritten to equations (A.0.4) and (A.0.5)

$$\frac{1}{2}mv_i^2 + \frac{1}{2}mv_j^2 = \frac{1}{2}mv_i'^2 + \frac{1}{2}mv_j'^2 + \Delta U \quad (\text{A.0.3})$$

$$v_i^2 - v_i'^2 + v_j^2 - v_j'^2 - \frac{2}{m}\Delta U = 0 \quad (\text{A.0.4})$$

$$(\mathbf{v}_i - \mathbf{v}'_i) \cdot (\mathbf{v}_i + \mathbf{v}'_i) + (\mathbf{v}_j - \mathbf{v}'_j) \cdot (\mathbf{v}_j + \mathbf{v}'_j) - \frac{2}{m}\Delta U = 0 \quad (\text{A.0.5})$$

Equation (A.0.2) can now be substituted into (A.0.5) to give equation (A.0.6).

$$\frac{A}{m}\hat{\mathbf{r}}_{ij}(\mathbf{v}_j - \mathbf{v}_i + \mathbf{v}'_j - \mathbf{v}'_i) - \frac{2}{m}\Delta U = 0 \quad (\text{A.0.6})$$

Equation (A.0.2) and the definition of the separation velocity vector ($\mathbf{v}_{ij} = \mathbf{v}_i - \mathbf{v}_j$) can be substituted into equation (A.0.6) to give (A.0.7).

$$-\frac{A^2}{m} - A\hat{\mathbf{r}}_{ij} \cdot \mathbf{v}_{ij} - \Delta U = 0 \quad (\text{A.0.7})$$

This is a quadratic equation in terms of A therefore it's roots must be given by equation (A.0.8).

$$A = -\frac{m}{2} \left((\mathbf{v}_{ij} \cdot \hat{\mathbf{r}}_{ij}) \pm \sqrt{(\mathbf{v}_{ij} \cdot \hat{\mathbf{r}}_{ij})^2 - \frac{4}{m} \Delta U} \right) \quad (\text{A.0.8})$$

From equation (A.0.2), the change in velocity of each particle is given in equations (A.0.9)

$$\Delta \mathbf{v}_i = \frac{A}{m} \hat{\mathbf{r}}_{ij} \quad (\text{A.0.9a})$$

$$\Delta \mathbf{v}_j = -\frac{A}{m} \hat{\mathbf{r}}_{ij} \quad (\text{A.0.9b})$$